BIAXIAL EXCITATION GENERATOR (BEGA) – 9 PHASES OPERATION IN FAULTY CONDITIONS

ADRIAN-DANIEL MARTIN [1], LIVIU-DANUT VITAN [2], LUCIAN TUTELEA [3], ION BOLDEA [4]

This paper presents a biaxial excitation generator for automobiles (BEGA) in generator mode, three three-phase windings (9 phases), and three diode bridge rectifiers DC parallel-connected for full power. BEGA is a synchronous machine with a biaxial excitation: one along the d-axis produced by the DC excitation coils (fed through brushes or contactless) and another along the q-axis produced by the PMs. The experimental demonstration of fault-tolerant characteristics was conducted under various fault conditions, including interrupted phases, short-circuited coils, and missing or short-circuited diodes. The importance of having all three three-phase windings (star-connection) connected in neutral points is highlighted and discussed. A fast Fourier transform presents a comprehensive analysis of the impact of these faults on the harmonic spectrum.

1. INTRODUCTION

Over the last few years, the interest in multiphase winding machines has been growing due to the demand for high fault-tolerance capability and high-power rating in safety-critical applications such as the aerospace, aviation, marine ship industry, medical industry, and nuclear power plants. Also, these machines are suitable in drive systems where long-term operation in faulty conditions is required for reasons such as difficult servicing and human access (*i.e*., offshore wind turbines, ship power systems, and electric vehicles [1–4]. In most cases, the multiphase winding machine is used as an autonomous generator with constant AC or DC output voltage at variable speed. It maintains a high level of the provided power in case of failure for critical consumers.

Most of the configurations use an AC generator with full or fractional AC-DC-AC or AC-DC static power converters [5–7]. Besides these, in [8–10] configurations based on SG with full power diode rectifier and detailed excitation control to deliver DC output power at constant voltage for variable speed are presented.

Yet another category of schemes uses PM generators with hybrid excitation along the same axis as PMs (axis d) to increase or decrease the PM flux by ± excitation current and the emf according to load and speed in a close-loop manner [11–13].

Constructive details related to BEGA that was here investigated can be found in [14], where also FEM simulations are provided. In addition to the previous conference paper, here, the authors bring new insights related to BEGA fault tolerant characteristics in terms short circuit inside of the machine and open circuit and short circuit in diode bridge rectifier.

At unity power factor, as imposed approximately by the diode rectifiers and with PMs in axis q, the voltage regulation is overall smaller than usual in a DC excited synchronous generator, which is crucial for keeping a certain DC output voltage with load and for a variable speed range (not explored here). The further exposed results of BEGA as a generator in fault condition (only one fault studied at the time) guarantee continuous and uninterrupted functionality and performances.

The main contributions of this paper which extends [14], are based on the demonstration of the fault tolerance characteristic of the BEGA structure (as a generator) in a multitude of operating conditions: 1) the fault occurred in the three-phase rectifier, 2) the fault occurred inside the machine. The paper continues as follows: the setup configuration and lab prototype description (2), experimental work (3), discussions on experimental results (4), conclusions (5)

2. SETUP CONFIGURATION AND LAB PROTOTYPE DESCRIPTION

The studied machine (BEGA) is loaded at a constant speed using a 5.5 kW induction machine driven by a four-quadrant variable frequency converter. In Fig. 1, the experimental setup can be seen, and Fig. 2 presents the experimental connection diagram of the BEGA machine.

In the lower left of Fig. 1, all the three-phase rectifier bridges and the DC filter capacitor (235 μF) can be seen. The generator was loaded using a resistive load. The measurements involved two synchronized oscilloscopes, each with four channels; seven measurements were performed simultaneously considering one synchronization channel.

A DC source ensures generator excitation. Each phase of each three-phase connection is composed of two serial-connected coils.
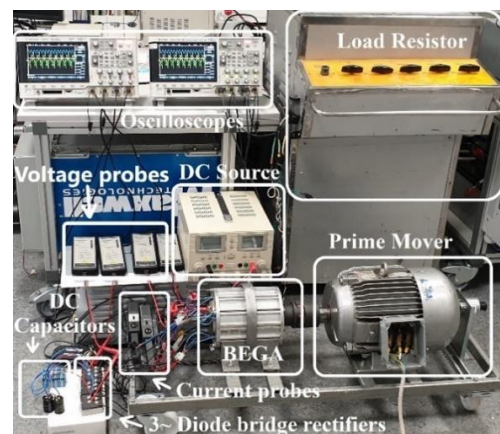

Fig. 1 – Laboratory experimental setup.

This way, the machine has three star-connected three-phase windings. Each three-phase winding is connected to a three-phase diode bridge rectifier (R1, R2, R3). All rectifiers are parallel connected on the DC side.

[1,2] University Politehnica Timisoara, Timisoara, Romania
[3] University Politehnica Timisoara and Romanian Academy Timişoara Branch, Timisoara, Romania
[4] Romanian Academy Timisoara Branch, Timişoara, Romania
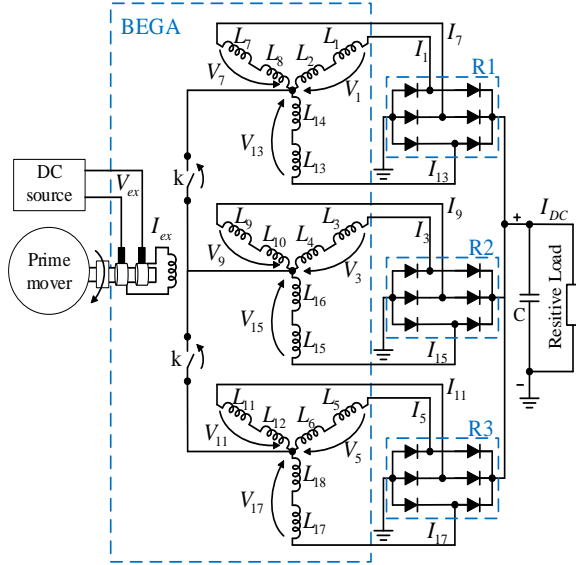 E-mails: adrian.martin@upt.ro, danut.vitan@upt.ro, lucian.tutelea@upt.ro, ion.boldea@upt.ro

Fig. 2 – Experimental connection diagram – BEGA with three three-phase windings connected to three diode bridge rectifiers.

Two separate cases are presented, each differing significantly in terms of redundancy: one with a common null (when contactor k is closed) and the other with an insulated null (when contactor k is open) – see Fig. 2. In both cases, experimental results are presented for no-fault and fault operation, with and without DC -filter when: one phase is missing (coil L_7+L_8), two phases are missing (coils L_7+L_8 and L_9+L_{10}) and three phases are missing (coils L_7+L_8, L_9+L_{10} and $L_{11}+L_{12}$).

3. EXPERIMENTAL WORK

Considering the large number of tests, Table 1 presents a summary of all experiments. All tests are performed at 2 400 rpm.

Table 1

Summary of the experimental work, based on the fault type

Conditions	Figures		FFT
	Unfiltered	Filtered	
No fault operation	8, 9	10	11
Internal machine fault			
One missing phase	12	18	
Two missing phases	13	19	
Three missing phases	14	20	18, 24
Two missing phases of the same three-phase winding	15	22	
One coil short-circuited	16	17, 23	
Diode bridge rectifier fault			
One open diode	27	–	–
One short-circuited diode	28	–	

Figure 3 presents induced voltage V_1 (on L_1+L_2 coils) measured in no-load and no-fault conditions for different excitation currents, with common null.

In the following, three different situations, each with specific results and analysis are given:

A) No-fault operation (with and without DC filtering) – the results are presented for a fully operational regime, when no faults are present, this case is used mainly for comparison with the fault-condition results.

B) Internal machine fault operation (with and without DC filtering) – when one coil is short-circuited or when one or multiple phases are missing.

C) Diode bridge rectifier fault operation – when one diode (of the three-phase diode bridge rectifier) is short-circuited or is missing.
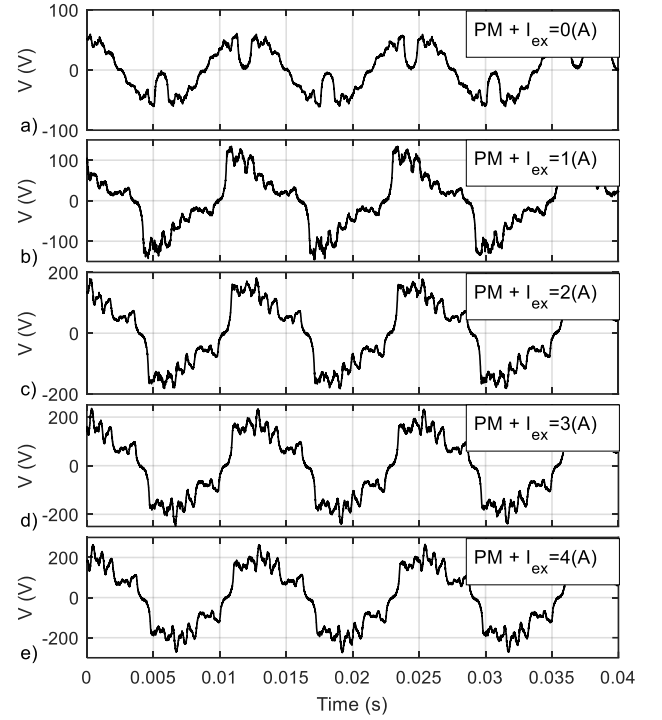

Fig. 3 – Phase voltage for no-load conditions with a common null:
a) by permanent magnet without excitation current (I_{ex} = 0 A) and
b), c), d), e) by permanent magnet with different excitation currents
$I_{ex} \in \{1,2,3,4\}$A – measurements.

In Fig. 4 and Fig. 5, the differences are illustrated between the common star connection of all three-phase windings (a and b) and an insulated neutral connection between them (c and d) under load and no-fault conditions, with a rated excitation current of 4 A, both with and without DC filtering.
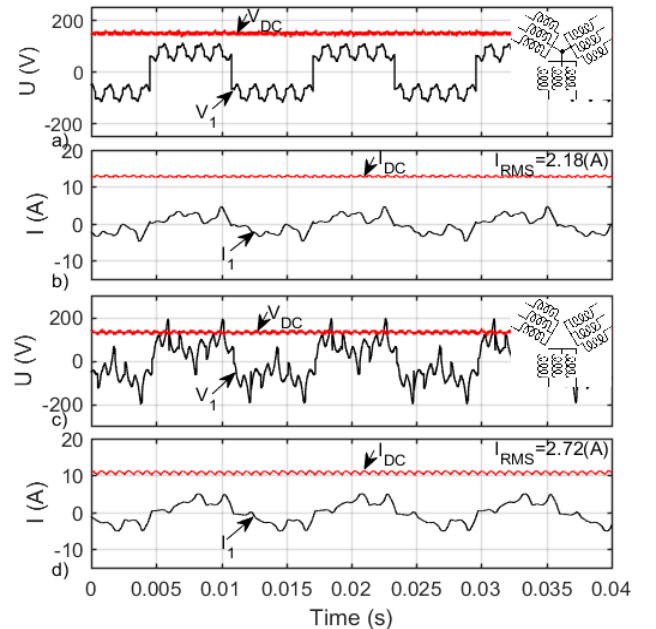

Fig. 4 – Phase and DC voltages and currents in load and no-fault conditions at rated excitation current with common null P_{DC} = 1 893 W, and with insulated null P_{DC} = 1 408 W – measurements.

In the top right-side corner of the figures, the type of connection is visually represented (with and without a common null connection). V_1 is measured on a phase obtained from L_1 and L_2 coils, and V_1 is the current that flows through it.
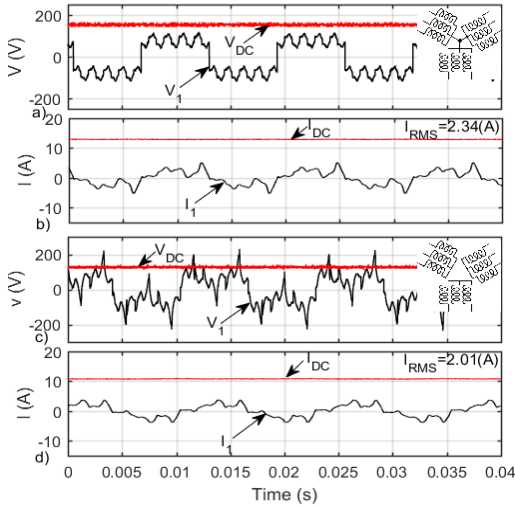
Fig. 5 – Phase and DC voltages and currents in load and no-fault conditions with 235 µF DC -filter at rated excitation current:
a), b) common null P_{DC} = 1 978 W, and
c), d) insulated null P_{DC} = 1 373 W – measurements.

When the DC filter is added with common null, for no-fault conditions (Fig. 6b), the high-frequency harmonics almost disappear, compared with no DC filter (Fig. 6a). The 2400 rpm rotor speed corresponds to 40 Hz rotor frequency. For 2 pole pairs, the electrical frequency is 80 Hz. After the rectifier, the DC voltage ripple frequency will be twice the frequency of the input voltage. With 9 phases/pole, the first significant harmonic is at 1 440 Hz.
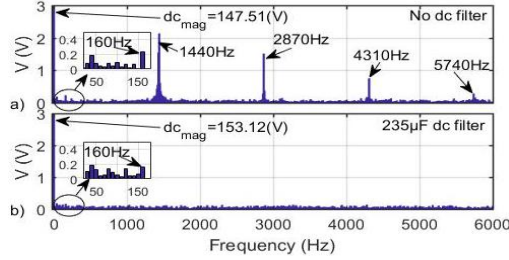

Fig. 6 – Fast Fourier Transform (FFT) on V_{DC} voltage with common null in no-fault and load conditions at rated excitation current:
a) without DC filter, b) with DC filter.

B. INTERNAL MACHINE FAULT OPERATION (WITHOUT AND WITH DC FILTERING)

In this case, BEGA was investigated for internal faults. Figure 7 to Fig. 11 shows the operation of the generator in faulty conditions. In Fig. 7, the measurements are recorded when one coil is missing from one three-phase winding (L_7 from rectifier R_1). In Fig. 8, two homologous coils from two different three-phase windings are missing and Fig. 9 presents the measurements when three homologous coils from three different three-phase windings are missing.

As shown in the authors' conference paper ([14] Fig. 15 and Fig. 16 – external characteristics), with and without fault, the DC voltage still decreases notably with the load at a constant DC excitation current. The common null connection ensures a higher output power in all presented cases.

In Fig. 10, BEGA has two missing coils of the same three-phase winding, while in Fig. 11 the machine has one short-circuited coil.

It can be observed in Figs. 10c, d, that with insulated null, the remaining phase on the faulty three-phase winding no longer influences the output generated power (phase current = 0). In these faulty conditions, with a common null connection

(Figs. 10a, b) the generated power is only 1.7% lower than the power generated in no-fault conditions (Figs. 4a, b), which leads to a high system redundancy. With insulated null, the generated power is 11% smaller than the power generated in no-fault conditions (Figs. 4c, d). So, the two missing phases of the same three-phase winding fault (Fig. 10) produces a bigger DC output power with a common null compared with the case when two phases of two different three-phase winding are missing (Fig. 8). Compared with no-fault conditions (Fig. 4) – as we expected – the DC output power is usually smaller in case of any type of defect. In Fig. 11, the measurements were recorded when the L_7 coil (Fig. 2) was short-circuited.

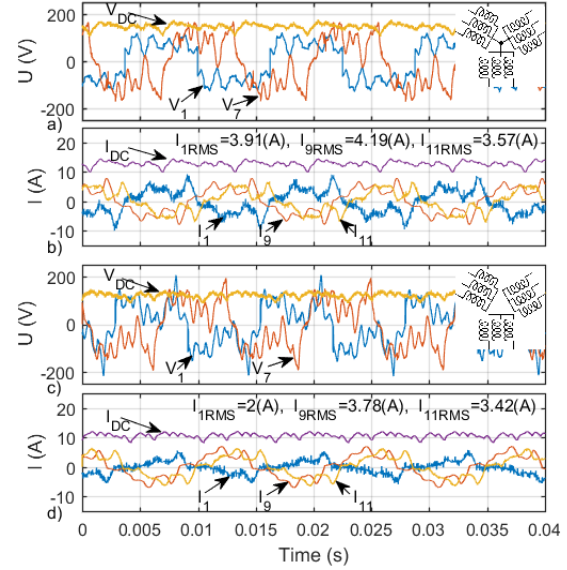### B.1. WITHOUT DC FILTERING
- One phase missing – no DC filter

Fig. 7 – Phase and DC voltages and currents in load conditions with coil L_7 missing, at rated excitation with: a), b) common null P_{DC} = 1880 W, and c), d) insulated null P_{DC} = 1 301 W – measurements.

The voltage on the interrupted phase and on neighboring phase on the same three-phase system has been measured. The currents on the phases next to the interrupted ones and the currents on the homologous phases of the other three-phase systems have been measured as well (Fig. 7 to Fig. 11).
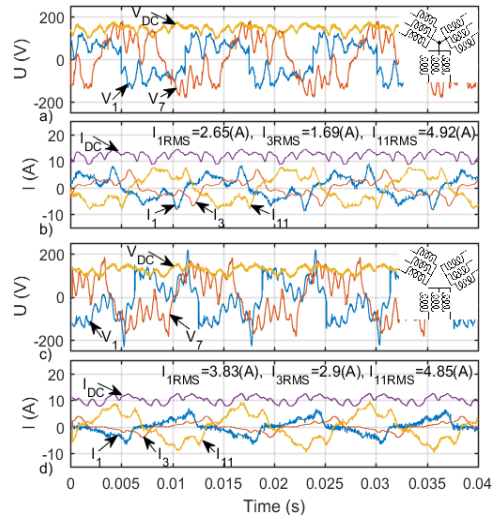
- Two phases missing – no DC filter

Fig. 8 – Phase and DC voltages and currents in load conditions with phases L_7, L_9 missing at rated excitation with: a), b) common null P_{DC} = 759 W, and c), d) insulated null P_{DC} = 1 301 W – measurements.
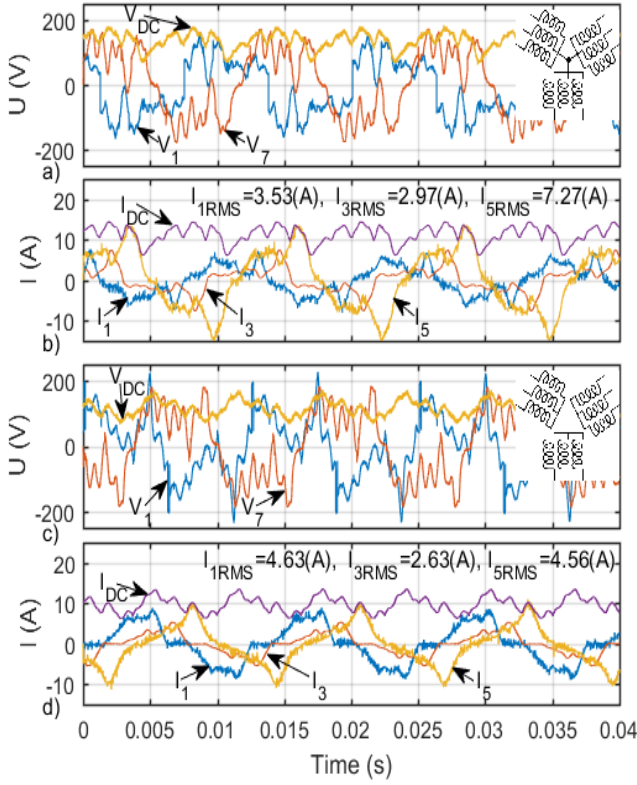
- Three phases missing – no DC filter

Fig. 9 – Phase and DC voltages and currents in load conditions with phases L_7, L_8, L_{11} missing at rated excitation current with:
a), b) common null $P_{DC} = 1\ 581$ W, and
c) d) insulated null $P_{DC} = 1\ 171$ W – measurements.

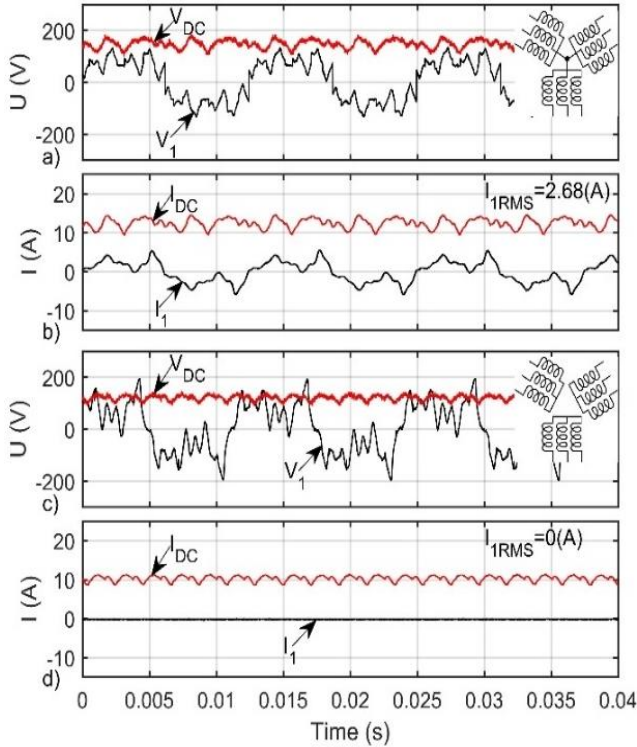- Two phases missing of the same three-phase winding – no DC filter

Fig. 10 – Phase and DC voltages and currents in load conditions with coils L_7, L_{13} missing of the same three-phase winding at rated excitation current with: a), b) common null $P_{DC} = 1\ 861$ W, and c) d) insulated null $P_{DC} = 1\ 253$ W – measurements.

- One coil short-circuited – no DC filtering

Figure 12 presents the FFT results obtained for internal machine fault conditions and no DC filter. Compared with Fig. 6a (FFT for unfiltered DC voltage in load and no-fault conditions – where the lower frequency from the frequency spectrum could be neglected), here, in faulty conditions, the lower frequency harmonics (160 Hz and 320 Hz) are dominant.
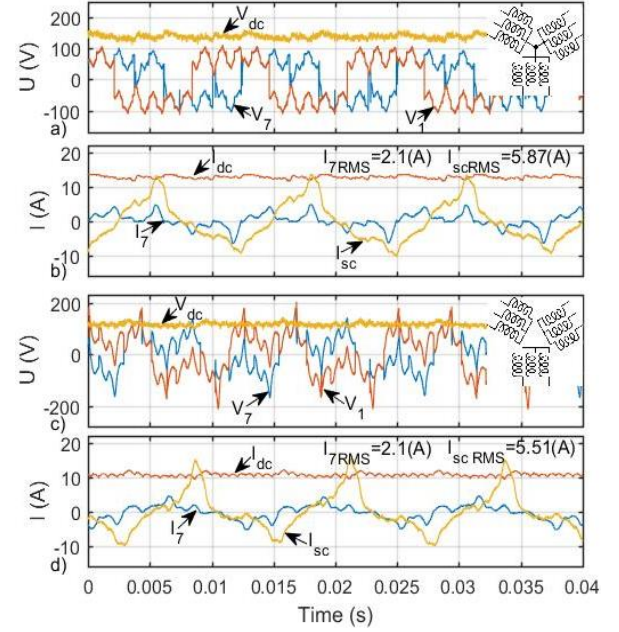

Fig. 11 – Phase and DC voltages and currents in load conditions with coil L_7 short-circuited at $I_{ex} = 4$ A with: a), b) common null $P_{DC} = 1\ 796$ W, and c) d) insulated null $P_{DC} = 1\ 236$ W (2 400 rpm) – measurements.
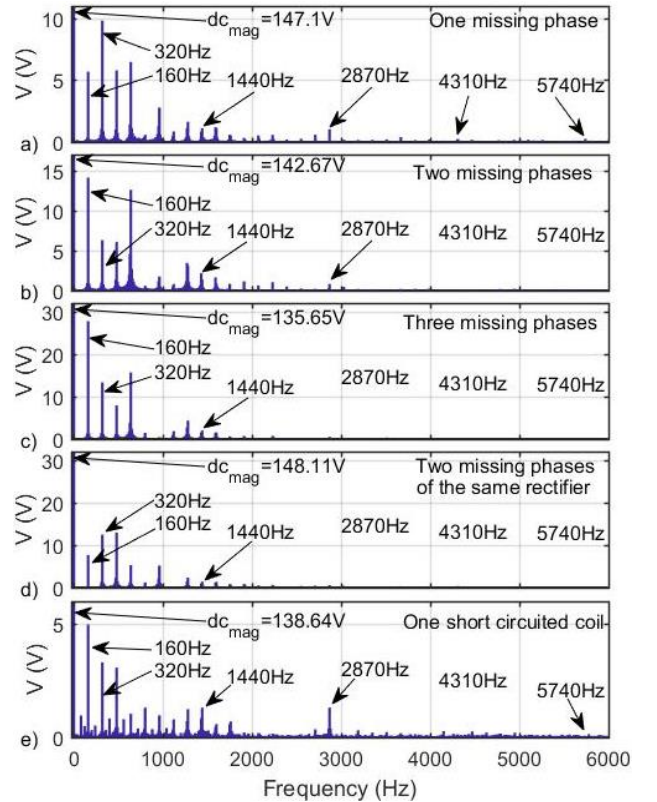

Fig. 12 – FFT on V_{dc} voltage with common null in load conditions (no DC filter) at $I_{ex} = 4$ A for a) coil L_7 missing, b) coils L_7, L_9 missing, c) coils L_7, L_9, L_{11} missing, d) coils L_7, L_{13} missing (of the same three-phase winding), e) coil L_7 short-circuited – measurements.

B. 2. WITH DC FILTERING

The DC voltage filtering effects are studied in the following figures (Fig. 13 to Fig. 17).
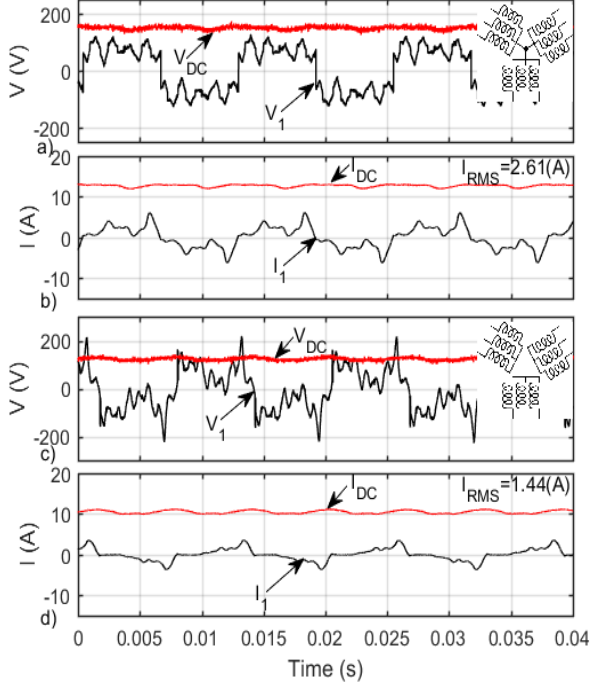
- One phase missing – with DC filter

Fig. 13 – Phase and DC voltages and currents in load conditions and coil L_7 missing with 235 µF DC-filter at rated excitation current with: a), b) common null P_{DC} = 1 908 W and c), d) insulated null P_{DC} = 1 290 W – measurements.

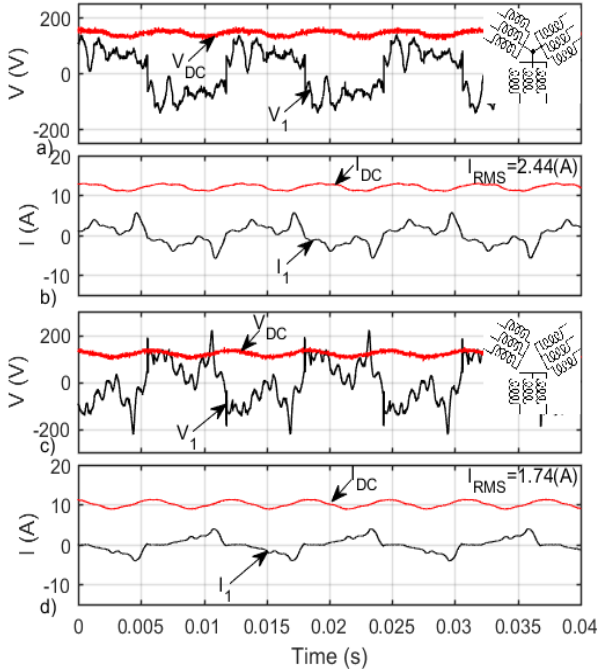- Two phases missing – with DC filter

Fig. 14 – Phase and DC voltages and currents in load conditions and coils L_7, L_9 missing with 235 µF DC-filter at rated excitation with: a), b) common null P_{DC} = 1 726 W and c), d) insulated null P_{DC} = 1 223 W – measurements.

From a redundancy point of view, in faulty conditions, the presence of the common null connection between all three-phase windings ensures a higher DC output power compared with the insulated null connection.

So far, with insulated null, the DC voltage has larger peak variations, and the output power is smaller, even if the phase RMS current is bigger.
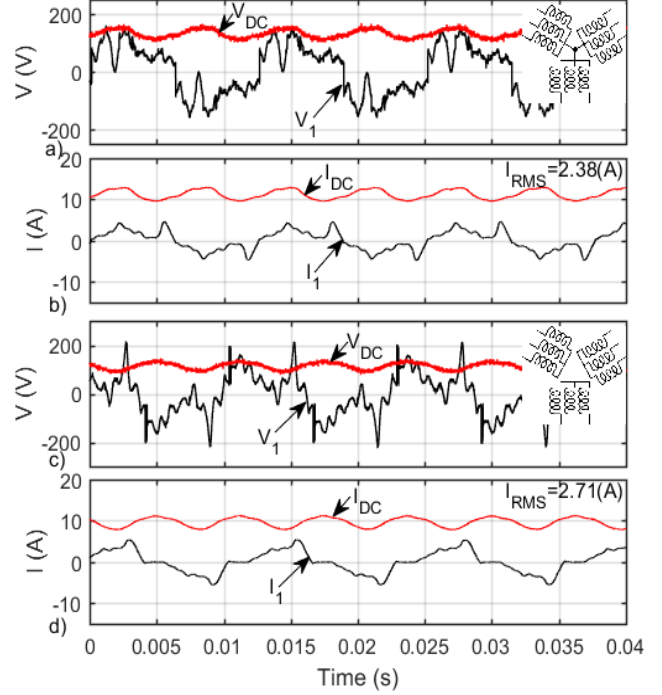
- Three phases missing – with DC filter

Fig. 15 – Phase and DC voltages and currents in load conditions and coils L_7, L_9, L_{11} missing with 235 µF DC-filter at rated excitation current with: a), b) common null P_{DC} = 1486 W and c), d) insulated null P_{DC} = 1 111 W – measurements.

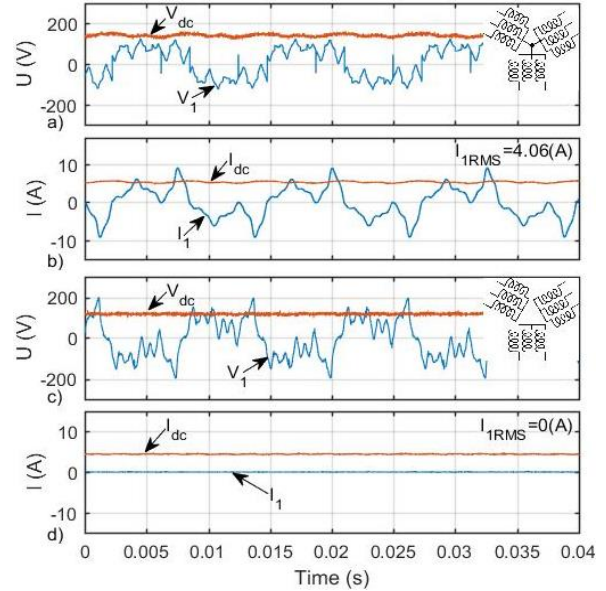- Two phases missing of the same three-phase winding – with DC filter

Fig. 16 – Phase and DC voltages and currents in load conditions with coils L_7, L_{13} missing of the same three-phase with 235 µF DC-filter at rated excitation current with: a), b) common null P_{DC} = 1 880 W and c) d) insulated null P_{DC} = 1 293 W – measurements.

With the DC filter, the test conditions were the same as in Fig. 7 to Fig. 11, with and without common null, where no DC -filter was used: one missing phase, two missing phases, three missing phases, two missing phases of the same three-phase winding and one coil short-circuited.
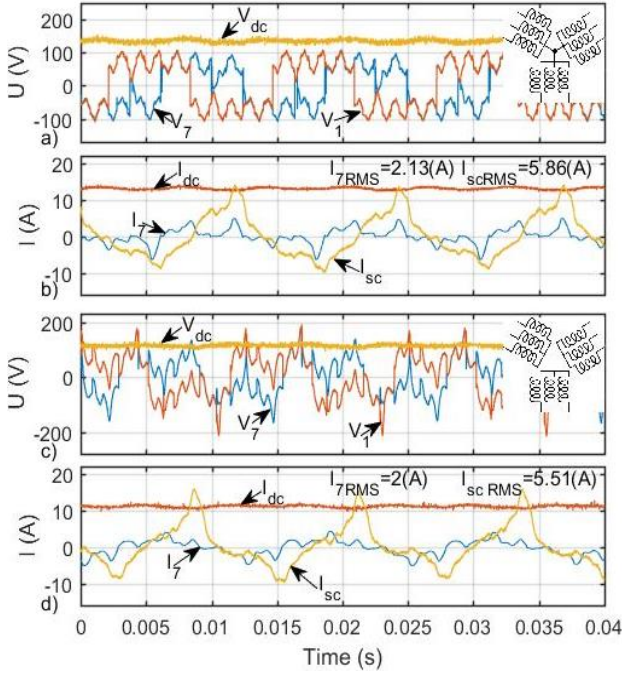
- One coil short-circuited – with a DC filter

Fig. 17 – Phase and DC voltages and currents in load conditions with coil L_7 short-circuited with 235 μF DC-filter at $I_{ex} = 4$ A with: a), b) common null $P_{DC} = 1\ 763$ W and c) d) insulated null $P_{DC} = 1\ 263$ W (2 400 rpm) – measurements.

Compared to Fig. 12 where the FFT results were presented in case of fault conditions and no DC filter, here (Fig. 18), for the same fault conditions and with a DC filter, the FFT results are shown.

Besides that, the output power changes, other effects of DC filtering are presented in Fig. 19; it can be observed that the frequency spectrum is cleared, so that the only significant harmonics are at 160 Hz and 320 Hz.

With the DC filter capacitor, as the number of missing phases increases, the 160 Hz frequency (second harmonic) becomes the predominant harmonic, while the higher frequency ones are eliminated. In these conditions, the measured current is only the load current, not containing the capacitor current.

When the DC filter is added (Fig. 6b), with common null, for no fault conditions, the high-frequency harmonics almost disappear, compared with no DC filter.

The signals were filtered for values smaller than 0.17 V.

Figure 19 shows the output power variations in different operation conditions (collected from Fig. 4 and Fig. 5, Fig. 7 to Fig. 11, and Fig. 13 to Fig. 17), both with common and insulated null, with and without DC filter.

With insulated null, with and without DC filtering the DC power is about 27% lower than the common null connection for all operating conditions.

In both cases (common and insulated null), without DC filtering, with a missing phase in all three three-phase windings (experiment number 3 in Fig. 19), the generator can still provide 83% of the no-fault system power.

It can be observed that BEGA presents high redundancy for two phases of the same three-phase winding fault conditions. This way, the DC output power is 98% with common null and 89% with insulated null.
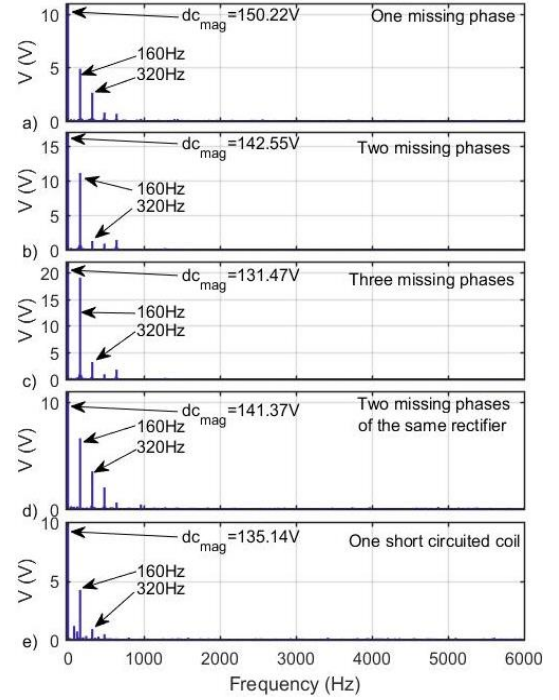

Fig. 18 – FFT on V_{DC} voltage with common null in load conditions with 235 μF DC-filter at $I_{ex} = 4$ A for a) coil L_7 missing, b) coils L_7, L_9 missing, c) coils L_7, L_9, L_{11} missing, d) coils L_7, L_{13}, missing (of the same three-phase winding), e) coil L_7 short-circuited – measurements.
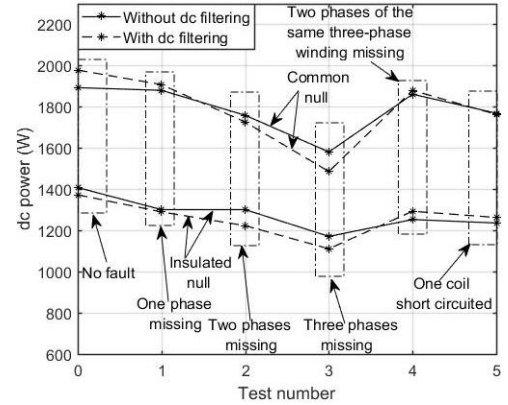

Fig. 19 – The fault impact on the DC-output power – with common and insulated null with and without dc filtering (2 400 rpm).

The relative harmonic content of the DC voltage (presented in Table 2) was calculated according to formula number 1, in different operating conditions with and without a DC filtering capacitor, with a common null.

$$RCH = \frac{\sqrt{\sum_{i=2}^{n} X_i^2}}{X_{1^{st}_{DC}}^2}, \qquad (1)$$

where X_i represents the filtered amplitude of each FFT value, n represents the number of samples and $X_{1^{st}_{DC}}^2$ represents the first FFT DC voltage component.

Table 2
Relative DC Voltage Harmonics Content (RHC)

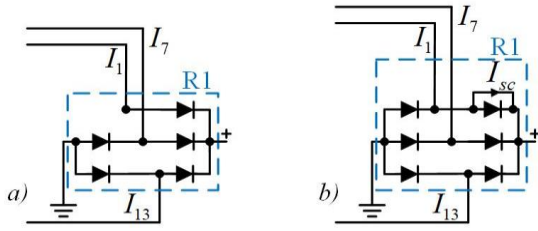| Tests	Without DC Capacitor	With DC Capacitor
No-fault conditions	1.66 %	0.33 %
One phase missing	7.47 %	2.69 %
Two phases missing	11.5 %	5.63 %
Three phases missing	19.23 %	10.47 %
Two phases missing of the same three-phase winding	10.55 %	3.9 %
One coil short-circuited	4.13 %	2.4 %

Fig. 20 – Zoom on Fig. 2: a) one open diode, b) one short-circuited diode.

C. DIODE BRIDGE RECTIFIER FAULT

In Fig. 20, the electrical diagram for the following two fault situations is presented: a) when one diode is open, b) one diode is short-circuited. With one open diode, the BEGA operation is almost unchanged compared to the internal machine fault operation. In Fig. 21, the results in this condition are presented in both cases: with and without a common null connection. The test was performed at rated loading and rated excitation current. The current I_1 (which flows through the remaining diodes in the faulty diode bridge rectifier leg) has a half-wave pattern, but even so, the generator was able to deliver 98.9% of its no-fault rated power.

Figure 22 presents the results for one short-circuited diode in no-load conditions in both, with and without insulated null.
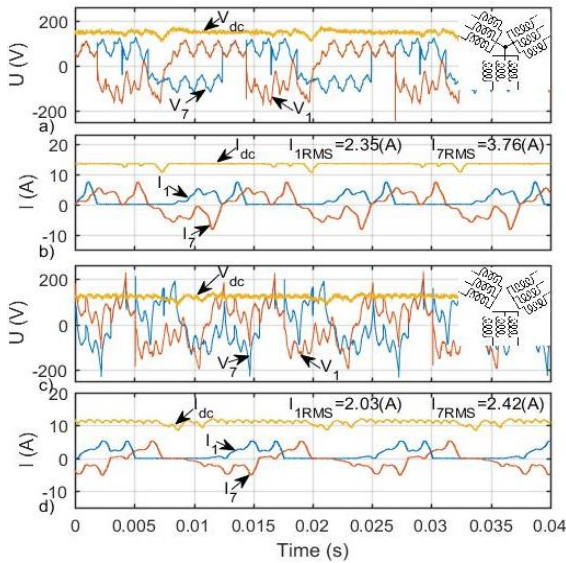
- One open diode

Fig. 21 – Phase and DC voltages and currents in load conditions and one open diode (see Fig. 20 and Fig. 21) at rated excitation current with: a), b) common null P_{DC} = 1872 W and c) and d) insulated null P_{DC} = 1320 W – measurements.

- One short-circuited diode

As can be seen from Fig. 22, with a common null connection, this fault produces very high currents, even if there is no excitation current.

The DC source used for excitation can be damaged: an alternating voltage is induced in excitation winding, with a 2.1 V RMS value. While the DC excitation source is still connected, an unwanted current starts to flow from excitation winding through the DC source (see Fig. 22).

In contrast to all the previous results, for this last faulty operation condition (with one short-circuited diode), the common null connection diagram produces worse results compared to the insulated null connection.
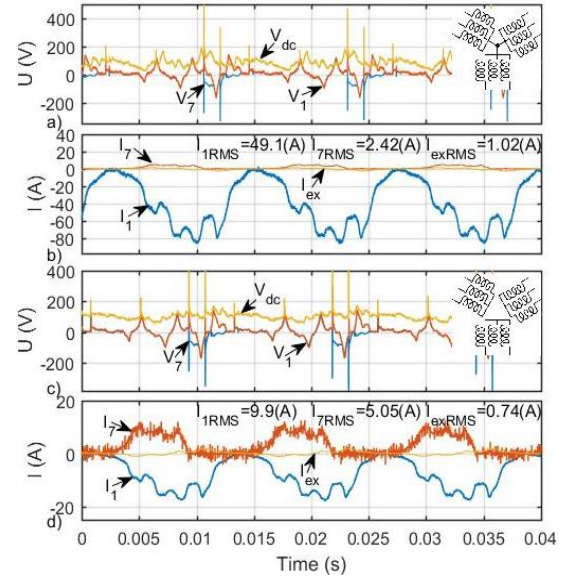

Fig. 22 – Phase and DC voltages and currents in no-load conditions and one short-circuited diode Fig. 20 and Fig. 21), no excitation with: a), b) common null and c), d) insulated null – measurements.

As the common null connection produces more power in faulty operation, special measures must be taken to prevent high additional excitation current for the shorted diode(s) faulty conditions.

4. **DISCUSSIONS ON EXPERIMENTAL RESULTS**

In section 3, BEGA was studied in no-fault (sub-section A) and faulty conditions (sub-sections B and C).

With a common neutral connection, high redundancy can be achieved under faulty conditions, such as when one phase is missing, one diode is open, or when two phases of the same three-phase winding are absent. Almost 99% of the no-fault rated power can still be produced in these scenarios without resulting in unbalanced stator currents.

The DC capacitor reduces the harmonic content on average by 55%, but without DC filtering, the highest relative harmonic content is found when three phases are missing (one of each three-phase winding); even so, the output power is still 83% of the no-fault generated power.

It was proved that with a common null connection, the generated power is almost 35% bigger than without a common null. On the other hand, in case of a common null connection in a faulty condition with one diode short-circuited, the generator produces high peak current values (short-circuit currents), which can damage the machine windings.

5. **CONCLUSIONS**

In this massively experimental paper, all tests were performed at a fixed speed of 2 400 rpm.

With connected null, in case of a single missing phase, the generator can still provide 99% of its power (Fig. 19). More than that, with two missing phases on the same three-phase winding, the generator can still provide 98% of its power (Fig. 19).

Although the voltage still drops significantly with loading at constant field current, in case of one missing phase in all three three-phase windings (three missing phases in total), BEGA can still provide approximately 83% of its no-fault condition power.

When all three-phase windings have a common null, about 35% more power can be generated than with insulated null connections.

BEGA presents high redundancy in the case of an open diode operation: it can deliver about 100% of the rated power with common null and about 94% of its rated power in the case of insulated null.

In the case of one short-circuited diode faulty condition, the corresponding phase current has unacceptable peak and RMS values. More than that, a dangerous induced voltage appears in the excitation winding, which can damage the DC-excitation source.

Given the promising performance of BEGA, a future investigation should be performed about optimal BEGA design to reduce further the voltage regulation, no-load voltage harmonics reduction, comprehensive digital simulation software that accounts for diode commutation, operation at variable speed and constant DC output voltage (with DC excitation closed-loop control).

ACKNOWLEDGMENTS

CREDIT AUTHORSHIP CONTRIBUTION STATEMENT

Author_1: Contribution to experiments, data processing, and writing
Author_2: Contribution to experiments and data processing
Author_3: Contribution to subject and state-of-the-art definition
Author_4: Contribution to subject and state-of-the-art definition

REFERENCES

1. S.-Y. Cherif, D. Benoudjit, M.-S. Nait-Said, N. Nait-Said, *Incipient short circuit fault impact on service continuity of an electric vehicle propelled by dual induction motors structure,* Rev. Roum. Sci. Techn. – Électrotechn. et Énerg.,**67**, *3*, pp. 265–270 (2022).

2. A.S. Abdel-Khalik, A.M. Massoud, S. Ahmed, *Nine-phase six-terminal induction machine modeling using vector space decomposition*, IEEE Trans. Ind. Electron., **66,** *2*, pp. 988–1000 (2019).

3. T. Roubache, S. Chaouch, *Nonlinear fault tolerant control of dual three-phase induction machines based electric vehicles*, Rev. Roum. Sci. Techn. – Électrotechn. et Énerg., **68**, *1*, pp. 65–70 (2023).

4. R. Belal, M. Flitti, M.L. Zegai, *Tuning of pi speed controller in direct torque control of dual star induction motor based on genetic algorithms and neuro-fuzzy schemes*, Rev. Roum. Sci. Tech. — Électrotechn. et Énerg., **69**, *1*, pp. 9–14 *(*2024).

5. S. Nuzzo, P. Bolognesi, G. Decuzzi, P. Giangrande, M. Galea, *A consequent-pole hybrid exciter for synchronous generators*, IEEE Trans. Energy Convers., **36**, *1*, pp. 368–379 (2021).

6. M. Niraula, L. Maharjan, B. Fahimi, M. Kiani, I. Boldea, *Variable stator frequency control of stand-alone DFIG with diode rectified output*, 5th International Symposium on Environment-Friendly Energies and Applications (EFEA), pp. 1–6 (2018).

7. F. Bu, H. Liu, W. Huang, H. Xu, Y. Hu, *Recent advances and developments in dual stator-winding induction generator and system*, IEEE Trans. Energy Convers., **33**, *3*, pp. 1431–1442 (2018).

8. L. Tutelea, I. Boldea, N. Muntean, S.I. Deaconu, *Modeling and performance of novel scheme dual winding cage rotor variable speed induction generator with DC link power delivery*, IEEE Energy Conversion Congress and Exposition (ECCE), pp. 271–278, 2014.

9. Y. Wu, L. Sun, Z. Zhang, Z. Miao, C. Liu, *Analysis of torque characteristics of parallel hybrid excitation machine drives with sinusoidal and rectangular current excitations*, IEEE Trans. Magn., **54**, *11*, pp. 1–5 (2018).

10. C. Ye, Y. Du, J. Yang, X. Liang, F. Xiong, W. Xu, *Research of an axial flux stator partition hybrid excitation brushless synchronous generator*, IEEE International Magnetics Conference (INTERMAG), pp. 1–1, 2018.

11. L. Tutelea, D. Ursu, I. Boldea, S. Agarlita, *IPM claw-pole alternator system for more vehicle braking energy recuperation*, J. Electr. Eng., **12**, pp. 211–220 (2012).

12. C. Stancu, T. Ward, K. Rahman, R. Dawsey, P. Savagian, *Separately excited synchronous motor with rotary transformer for hybrid vehicle application*, IEEE Energy Conversion Congress and Exposition (ECCE), pp. 5844–5851 (2014).

13. G. Dajaku, B. Lehner, Xh. Dajaku, A. Pretzer, D. Gerling, *Hybrid excited claw pole rotor for high power density automotive alternators*, XXII International Conference on Electrical Machines (ICEM), pp. 2536–2543, 2016.

14. A.D. Martin, L.D. Vitan, I. Torac, L.N. Tutelea, I. Boldea, *BEGA-biaxial excitation generator – operation for constant diode dc output voltage with 3,6,9 phases for increased redundancy*, International Aegean Conference on Electrical Machines and Power Electronics (ACEMP), International Conference on Optimization of Electrical and Electronic Equipment (OPTIM), pp. 383–390, 2021.